

## Spin-inversion in nanoscale graphene sheets with a Rashba spin-orbit barrier

Somaieh Ahmadi, Mahdi Esmailzadeh, Esmail Namvar, and Genhua Pan

Citation: *AIP Advances* **2**, 012130 (2012); doi: 10.1063/1.3684600

View online: <http://dx.doi.org/10.1063/1.3684600>

View Table of Contents: <http://aipadvances.aip.org/resource/1/AAIDBI/v2/i1>

Published by the [American Institute of Physics](http://www.aip.org).

---

### Related Articles

Aharonov-Bohm effect in an electron-hole graphene ring system

*Appl. Phys. Lett.* **100**, 203114 (2012)

Exceptional high Seebeck coefficient and gas-flow-induced voltage in multilayer graphene

*Appl. Phys. Lett.* **100**, 183108 (2012)

Hydrodynamic model for electron-hole plasma in graphene

*J. Appl. Phys.* **111**, 083715 (2012)

Snake states and Klein tunneling in a graphene Hall bar with a pn-junction

*Appl. Phys. Lett.* **100**, 163121 (2012)

Conductance oscillation of graphene nanoribbon with tilted p-n junction

*J. Appl. Phys.* **111**, 083708 (2012)

---

### Additional information on AIP Advances

Journal Homepage: <http://aipadvances.aip.org>

Journal Information: <http://aipadvances.aip.org/about/journal>

Top downloads: [http://aipadvances.aip.org/most\\_downloaded](http://aipadvances.aip.org/most_downloaded)

Information for Authors: <http://aipadvances.aip.org/authors>

### ADVERTISEMENT

**NEW!**

**iPeerReview**  
AIP's Newest App



**Authors...  
Reviewers...  
Check the status of  
submitted papers remotely!**

**AIP | Publishing**

## Spin-inversion in nanoscale graphene sheets with a Rashba spin-orbit barrier

Somaieh Ahmadi,<sup>1,a</sup> Mahdi Esmaeilzadeh,<sup>2,b</sup> Esmail Namvar,<sup>3</sup> and Genhua Pan<sup>4</sup>

<sup>1</sup>Department of Physics, Iran University of Science and Technology, Narmak, Tehran 16844, Iran

<sup>2</sup>Department of Physics, Iran University of Science and Technology, Narmak, Tehran 16844, Iran

<sup>3</sup>Department of Physics, Tarbiat Moallem University, 49 Dr Mofatteh Avenue, Tehran 15614, Iran

<sup>4</sup>School of Computing and Mathematics, University of Plymouth, Plymouth, Devon, PL4 8AA, United Kingdom

(Received 3 November 2011; accepted 12 January 2012; published online 1 February 2012)

Spin-inversion properties of an electron in nanoscale graphene sheets with a Rashba spin-orbit barrier is studied using transfer matrix method. It is found that for proper values of Rashba spin-orbit strength, perfect spin-inversion can occur in a wide range of electron incident angle near the normal incident. In this case, the graphene sheet with Rashba spin-orbit barrier can be considered as an electron spin-inverter. The efficiency of spin-inverter can increase up to a very high value by increasing the length of Rashba spin-orbit barrier. The effect of intrinsic spin-orbit interaction on electron spin inversion is then studied. It is shown that the efficiency of spin-inverter decreases slightly in the presence of intrinsic spin-orbit interaction. The present study can be used to design graphene-based spintronic devices. *Copyright 2012 Author(s). This article is distributed under a Creative Commons Attribution 3.0 Unported License.* [doi:10.1063/1.3684600]

### I. INTRODUCTION

Graphene, a single layer of carbon atoms packed into a two-dimensional honeycomb network, has attracted enormous research interests in recent years because of its fascinating properties such as room temperature quantum Hall effect,<sup>1-3</sup> excellent electrical and thermal conductivities,<sup>4-10</sup> ballistic carrier transport,<sup>11,12</sup> superior mechanical strength and flexibility,<sup>13,14</sup> and high sensitivity to adsorbed chemicals.<sup>15,16</sup> In recent experimental studies, it has been shown that the electron spin-relaxation length in graphene is very long (of the order of  $1\mu\text{m}$  at room temperature).<sup>17-20</sup> As a result, graphene is a promising candidate for spintronic devices. Spin-dependent electron transport in graphene has been studied vastly in recent years (see e.g., Refs. 21-28).

Although graphene is not intrinsically a ferromagnet,<sup>29-32</sup> ferromagnetic behavior and spin polarized states can be created by putting graphene in close proximity to a magnetic insulator such as EuO.<sup>30-32</sup> Also, spin-orbit interaction (SOI) can be used to obtain spin polarized states and to manipulate the spin of electrons in graphene. There are two kinds of SOI in graphene: the intrinsic SOI and the Rashba (extrinsic) SOI. Intrinsic SOI, which is induced by carbon intra-atomic spin orbit coupling, can open a gap in graphene energy dispersion and it can also convert graphene into a topological insulator with fractional spin Hall effect.<sup>33</sup> Intrinsic SOI is very small in a clean and flat graphene. The calculated value of intrinsic SOI is in the range of 0.0011-0.05 meV.<sup>34,35</sup> On the other hand, the value of Rashba SOI, which is induced by interaction of carbon atoms with the

<sup>a</sup>Electronic mail: [s\\_ahmadi@iust.ac.ir](mailto:s_ahmadi@iust.ac.ir)

<sup>b</sup>Electronic mail: [mahdi@iust.ac.ir](mailto:mahdi@iust.ac.ir)



substrate, has been reported to be up to 1 meV.<sup>33,34,36</sup> Dedkov *et al.* have shown experimentally that the Rashba spin splitting increases up to a very large value (i.e., 200 meV) by depositing graphene on a Ni (111) substrate.<sup>37</sup> The value of Rashba spin splitting reported by Dedkov *et al.* was soon challenged by Rader *et al.*<sup>38</sup> In an experimental study, Varykhalov *et al.* have reported the interaction of Au atoms between the graphene and Ni substrate can enhance the Rashba spin splitting to a large value of order 13 meV.<sup>39</sup> Recently, using density functional theory, Li *et al.* have shown that the Rashba splitting can be increase up to near 100 meV by depositing graphene on Au substrate.<sup>40</sup> The impurities effect on inducing spin-orbit coupling in graphene has been studied by Castro-Neto and Guinea.<sup>41</sup> They found that the spin-orbit coupling induced by impurities can be comparable to what found for zinc-blende semiconductors.

Manipulating the spin degree of freedom of electrons is an important subject in spintronics. The electron spin inversion is one of the main purposes of spin manipulation. Spin inversion in semiconductors has been studied extensively, but there are few studies in nanoscale semiconductors (see Refs. 42 and 43). In Ref. 42, Cardoso and Pereyra have used two semiconductor magnetic superlattices to invert the spin of electron. In the first superlattice the spin of the larger fraction (about 80%) of incoming electrons are inverted and then the second superlattice filters those electrons which are not inverted in the first superlattice. The spin-inverter proposed by Cardoso and Pereyra is complicated because it needs two stages for a complete spin inversion. Also, tuning of electron energy, in practice, is not easy because the spin inversion occurs at sharp resonance peaks. In Ref. 43, Busl and Platro have shown that a triple quantum dot under crossed dc and ac magnetic fields can act as spin-inverter by tuning the electric gate voltages of two dots. The limitation of this spin-inverter is that the inversion of both up and down spins does not occur at the same conditions. The efficiency of spin-inverter proposed by Cardoso and Pereyra is about 80%<sup>42</sup> and the efficiency of spin-inverter proposed by Busl and Platro has not been mentioned in their paper.<sup>43</sup> In a recent study, Fallah and Esmailzadeh have shown that, in the presence of proper Rashba spin-orbit strength, an organic (1,4-2phenyl-dithiolate) molecule can act as an electron spin inverter.<sup>44</sup> Although spin-dependent electron transport in graphene has been studied extensively in recent years,<sup>21–28</sup> to the best of our knowledge, electron spin inversion in graphene has not been studied.

The purpose of the present paper is to study the electron spin-inversion in nanoscale graphene sheets. It is shown that graphene sheets with a Rashba spin-orbit barrier can act as an electron spin-inverter. The spin-inversion occurs at the same condition (or Rashba SOI strength) for both up and down spins with very high efficiency. The graphene spin inverter is not complicated and needs no external magnetic or electric fields. The organization of this paper is as follows. In Sec. II, the Hamiltonian of an electron passing through the Rashba spin-orbit barrier is formulated and a theoretical model describing the spin-dependent transmission coefficient is then presented. In Sec. III, numerical results are presented and discussed. Section IV contains a summary and conclusion.

## II. THEORETICAL MODEL

Consider a nanoscale single sheet of graphene with a Rashba spin-orbit barrier or Rashba spin orbit region as shown in Fig. 1. We make the assumption that the dimensions of nanoscale graphene sheet are large enough to ignore its edge effects. Also, we assume ballistic transport as the electrons go through the Rashba barrier. Although the intrinsic SOI is small, for the sake of generality, we assume that there is an intrinsic SOI inside the Rashba spin-orbit barrier. Using the Kane-Mele model,<sup>45</sup> the Hamiltonian of an electron, in the presence of Rashba and intrinsic SOIs, can be written as

$$H = H_0 + H_I + H_R, \quad (1)$$

where

$$H_0 = -i\hbar v_f \psi^\dagger (\sigma_x \tau_z \partial_x + \sigma_y \partial_y) \psi, \quad (2)$$

is the Dirac Hamiltonian for massless fermions,<sup>45</sup>  $H_R$  and  $H_I$  are the Rashba and intrinsic SOIs, respectively. In Eq. (2),  $\hbar$  is the reduced Planck constant,  $v_f$  is the Fermi velocity in graphene,  $\sigma$  and

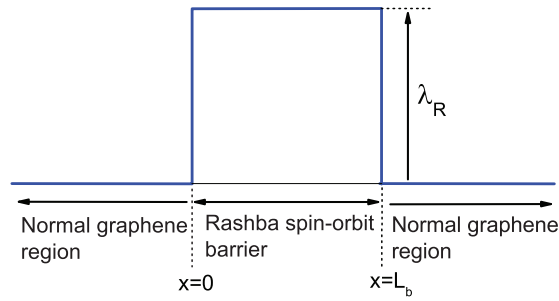


FIG. 1. (Color online) Schematic illustration of a Rashba spin-orbit barrier with height (or spin-orbit strength)  $\lambda_R$  and length  $L_b$ .

$\tau$  are Pauli spin matrices. The states on the A and B sublattices<sup>46</sup> and states at the Dirac points are described by  $\sigma_z = \pm 1$  and  $\tau_z = \pm 1$ , respectively. The slowly envelop function  $\psi(x, y)$ , in Eq. (2), is the Bloch wave function of electron. The Rashba SOI can be written as<sup>22,45</sup>

$$H_R = \frac{\lambda_R}{2} \psi^\dagger (\sigma_y s_x - \sigma_x \tau_z s_y) \psi, \quad (3)$$

where  $\lambda_R$  is the strength of Rashba SOI which considered here as barrier height and  $\mathbf{s}$  is Pauli matrix representing the spin of electron. The intrinsic SOI is given by<sup>22,45</sup>

$$H_I = \Delta \psi^\dagger \tau_z s_z \psi, \quad (4)$$

where  $\Delta$  is the strength of intrinsic SOI interaction and  $s_z$  is the  $z$  component of Pauli matrix.

Now, we consider an electron with energy  $E$  and spin  $s$  propagating from the left of graphene sheet to the Rashba barrier (see Fig. 1). Substituting Eqs. (2)–(4) into Eq. (1) and using transfer matrix method, the spin-dependent transmission coefficient can be obtained as<sup>47</sup>

$$T_{s \rightarrow s'} = \frac{1}{|w_{13}w_{31} - w_{11}w_{33}|^2} (|w_{31}\delta_{s,\uparrow} - w_{11}\delta_{s,\downarrow}|^2 \delta_{s',\uparrow} + |w_{33}\delta_{s,\uparrow} - w_{13}\delta_{s,\downarrow}|^2 \delta_{s',\downarrow}), \quad (5)$$

where  $T_{s \rightarrow s'}$  is the transmission coefficient for electron with incoming spin  $s$  and outgoing spin  $s'$ ,  $\delta_{s,s'}$  is the Kronecker delta,  $W_{ij}$  is  $ij$ th element of transfer matrix and

$$\mathbf{W} = [\mathbf{M}_N(0^-)]^{-1} [\mathbf{M}_{so}(0^+)] [\mathbf{M}_{so}(L_b^-)]^{-1} [\mathbf{M}_N(L_b^+)], \quad (6)$$

is the transfer matrix.<sup>47</sup> In Eq. (6),  $x^\pm \equiv x \pm \varepsilon$ ,  $x = 0(L_b)$  is the position of the left (right) normal/Rashba spin-orbit interface (see Fig. 1),  $\varepsilon$  is an infinitesimal positive number and the columns of  $4 \times 4$  matrix  $\mathbf{M}_{so}$  and  $\mathbf{M}_N$  can be determined by using the normalized eigenspinor of Eqs. (1) and (2) in the spin-orbit and normal regions, respectively.<sup>22</sup>

### III. RESULTS AND DISCUSSION

A numerical study of spin-inversion properties of a graphene sheet with a Rashba spin-orbit barrier is presented in this section using Eq. (5). The normalized Fermi energy is taken to be  $E_0 = 2$  in all numerical calculations. The spin-dependent transmission coefficients with spin-inversion (i.e.,  $T_{\downarrow \rightarrow \uparrow}$ ) and without spin-inversion or without spin change (i.e.,  $T_{\downarrow \rightarrow \downarrow}$ ) as a function of electron incident angle  $\theta$  are shown in Fig. 2 for an arbitrary Rashba spin-orbit strength or barrier height  $\lambda_R = 0.8$ . Here, the incoming electron is considered to be polarized with down spin state, the length of Rashba spin-orbit barrier is taken to be  $L_b = 100nm$ , and the intrinsic SOI is assumed to be very small (i.e.,  $\Delta \cong 0$ ). It is observed that, due to the Rashba SOI, the transmission coefficient with spin-inversion (i.e.,  $T_{\downarrow \rightarrow \uparrow}$ ) is not zero and has two peaks at incident angles  $\theta = \pm 48^\circ$ . At these

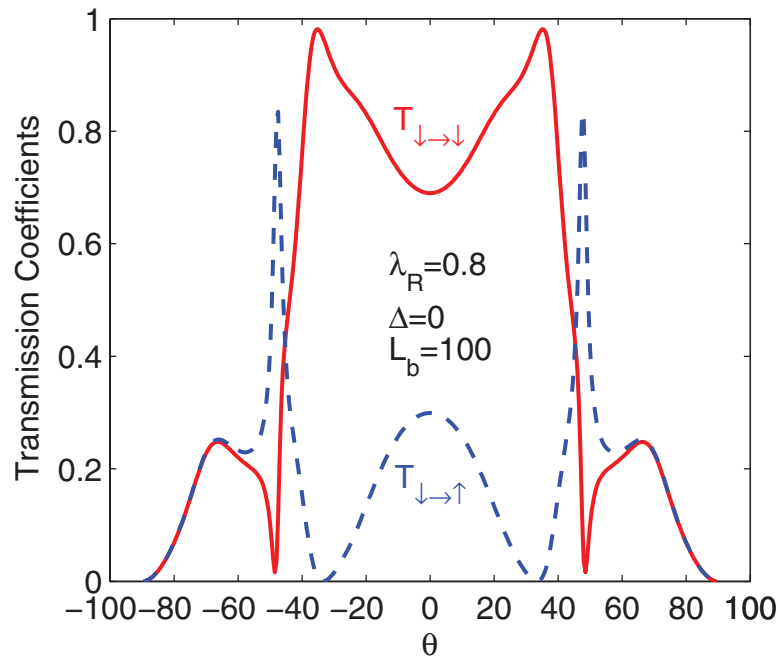


FIG. 2. (Color online) Electron transmission coefficient with spin-inversion ( $T_{\downarrow\rightarrow\uparrow}$ ) and without spin-inversion ( $T_{\downarrow\rightarrow\downarrow}$ ) as a function of electron incident angle  $\theta$  for an arbitrary Rashba barrier height  $\lambda_R = 0.8$ . The other parameters are shown in the figure.

angles, the transmission coefficient  $T_{\downarrow\rightarrow\uparrow}$  has a large value about 0.83 whereas the transmission coefficient without spin-inversion  $T_{\downarrow\rightarrow\downarrow}$  is very small about 0.02. Our numerical calculations show that, in the presence of Rashba spin-orbit barrier, the transmission coefficients with and without spin-inversion for incoming electron with up spin state are the same as those for incoming electron with down spin state (i.e.,  $T_{\uparrow\rightarrow\downarrow} = T_{\downarrow\rightarrow\uparrow}$  and  $T_{\uparrow\rightarrow\uparrow} = T_{\downarrow\rightarrow\downarrow}$ ). Thus the spin-dependent transmission properties for incoming electron with down and up spin states are the same and spin-inversion can take place at the same incident angles  $\theta = \pm 48^\circ$  for incoming electron with both down and up spin states. In the rest of the paper, we only study the transmission properties for incoming electron with down spin state.

As mentioned above, spin-inversion can be obtained in a graphene sheet with barrier height  $\lambda_R = 0.8$  at specific incident angles  $\theta = \pm 48^\circ$ . In this case, the system (graphene sheet with a Rashba SOI barrier) can be considered as an electron spin-inverter which is an important element in spintronic devices. The efficiency of spintronic devices is a significant factor in spintronics. The efficiency of spin-inverter can be defined as

$$\eta = (T_{s\rightarrow s'} - T_{s\rightarrow s}) \times 100. \quad (7)$$

where  $s' \neq s$ . As it is seen from Fig. 2, the efficiency of spin-inverter is equal to 81% at incident angles  $\theta = \pm 48^\circ$ . Although the efficiency is relatively high for these angles, the spin inversion occurs at nearly sharp peaks and at angles far from the normal incident  $\theta = 0^\circ$ . Also, spin-inversion is not perfect because the transmission coefficient without spin inversion (i.e.  $T_{\downarrow\rightarrow\downarrow}$ ) is not zero at these angles (see Fig. 2).

By changing the height of Rashba barrier, we can find proper conditions for electron spin-inversion at normal incident. Figure 3 shows the electron transmission coefficients with and without spin-inversion as a function of incident angle  $\theta$  for  $\lambda_R = 0.493$ . The other parameters are the same as those in Fig. 2. It is observed that, at normal incident and in a wide angular region about it (i.e.,  $-15^\circ < \theta < 15^\circ$ ), the transmission coefficient for electron with spin-inversion (i.e.,  $T_{\downarrow\rightarrow\uparrow}$ ) is very

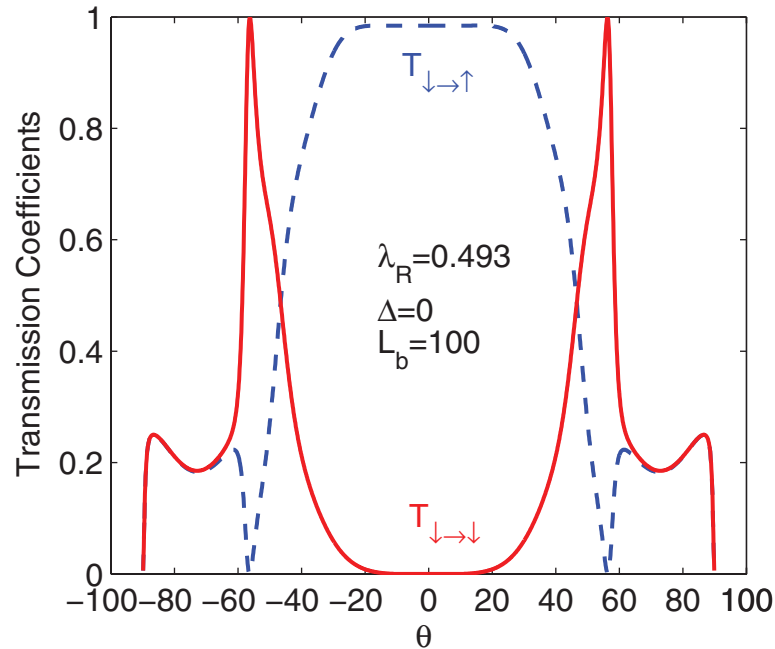


FIG. 3. (Color online) Electron transmission coefficients  $T_{\downarrow \rightarrow \uparrow}$  and  $T_{\downarrow \rightarrow \downarrow}$  as a function of electron incident angle  $\theta$  for Rashba barrier height  $\lambda_R = 0.493$  at which perfect spin inversion can occur. The other parameters are the same as those in Fig. 2.

close to 1, while the transmission coefficient for electron without spin change (i.e.,  $T_{\downarrow \rightarrow \downarrow}$ ) is zero. As a result, in this angular region, the complete spin-inversion from down to up and vice versa can take place and the graphene sheet with Rashba spin-orbit barrier can act as a perfect spin-inverter. In this case, as it is seen from Fig. 3, the efficiency of spin-inverter is very high (i.e.,  $\eta = 98.4\%$ ) for angular region  $-15^\circ < \theta < 15^\circ$ .

Note that the Rashba SOI acts like an effective magnetic field oriented along the y-direction. The spin of electrons moving along the x-direction rotates about y-direction due to this effective magnetic field. There is a characteristic length scale called spin precession length. For normal incident or for electrons moving along the x-direction, when the Rashba barrier length is equal to one half of spin precession length, the spin of electrons rotates  $180^\circ$  and thus spins along  $+z$  (up) invert to  $-z$  (down) and vice versa.

Figure 4 shows the transmission coefficients  $T_{\downarrow \rightarrow \uparrow}$  and  $T_{\downarrow \rightarrow \downarrow}$  as a function of incident angle  $\theta$  in the presence of intrinsic spin-orbit with strength  $\Delta = 0.2$ . The other parameters are the same as those in Fig. 3. As shown in this figure, spin inversion occurs at normal incident in the presence of intrinsic SOI but perfect spin-inversion does not take place at normal incident because there is a non zero transmission coefficient for electron without spin inversion (i.e.,  $T_{\downarrow \rightarrow \downarrow}$  is not zero). The efficiency of spin-inverter, in the presence of intrinsic SOI, is  $\eta = 92.3\%$  at normal incident which is about 6% less than that in the absence of intrinsic SOI. Comparing Figs. 3 and 4, it is observed that the mirror symmetry about  $\theta = 0^\circ$  is no longer valid in the presence of intrinsic SOI for transmission coefficient of electron with spin inversion  $T_{\downarrow \rightarrow \uparrow}$ . The symmetry breaking due to the intrinsic SOI is a well known effect (see e.g., Ref. 48). Since the intrinsic SOI in clean and flat graphene sheets is small and for the case in which the intrinsic SOI is not small it has no significant destructive effect on spin-inversion, we ignore it by setting  $\Delta = 0$  in the rest of the paper.

Now, we investigate the effect of barrier length on spin-inversion properties. Figure 5(a) shows the barrier height or Rashba strength  $\lambda_R$  as a function of barrier length  $L_b$  for perfect spin inversion.

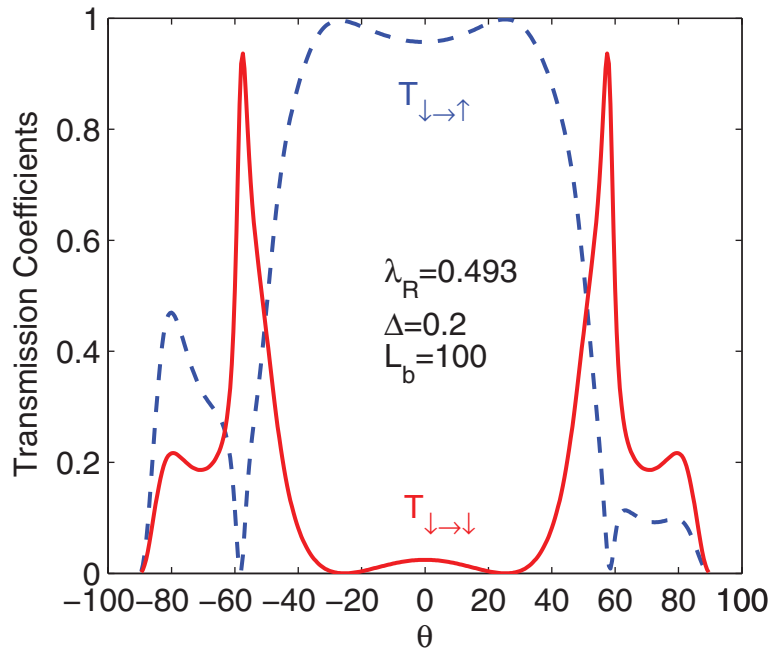


FIG. 4. (Color online) Electron transmission coefficients  $T_{\downarrow\rightarrow\uparrow}$  and  $T_{\downarrow\rightarrow\downarrow}$  in the presence of intrinsic SOI with  $\Delta = 0.2$ . The other parameters are the same as those in Fig. 3.

It is seen that the Rashba strength decreasing with increasing the barrier length. As a result, for a substrate with small Rashba SOI strength, one can increase the Rashba SOI region or barrier length to obtain perfect spin inversion. In Fig. 5(b), the efficiency of spin-inverter as a function of barrier length  $L_b$  is shown for perfect spin inversion. As we see in this figure, the efficiency has oscillatory behavior and has some maximums at which the efficiency reaches to 100%. The efficiency has also some minimums but the value of efficiency at minimums increases with increasing the barrier length. Therefore, the spin-inverter efficiency increases as the barrier length increases.

Up to now, we have considered a Rashba SOI barrier with perfectly sharp interfaces between the normal and SOI regions (see Fig. 1). The perfectly sharp interface may be seemed to be an unrealistic scenario. Although many works have been done with perfectly sharp interface to study other properties of spin-dependent electron transmission in graphene (see e.g., Refs. 22–24, 27), we consider a relatively realistic spin-orbit barrier with non-sharp interface (a trapezoidal barrier) and investigate the spin inversion properties of such a barrier. In Fig. 6(a), a trapezoidal barrier, with linearly increasing (decreasing) SOI strength in the left (right) of it, is shown. A rectangular barrier with its area is the same as the area of trapezoidal barrier is also shown in this figure. Figure 6(b) shows the electron transmission coefficient with spin inversion  $T_{\downarrow\rightarrow\uparrow}$  for trapezoidal and rectangular barriers corresponding to Fig. 6(a). As figure 6(b) shows, there are no significant differences for spin-inversion properties near the normal incident between the trapezoidal and rectangular barriers except the transmission coefficient  $T_{\downarrow\rightarrow\uparrow}$  and thus the efficiency of spin-inverter with trapezoidal barrier is slightly greater than those of rectangular one. The increment of efficiency may be due to the gradually varying of SOI strength at the interfaces of trapezoidal barrier.

In order to obtain perfect spin-inversion, the (normalized) Rashba SOI strength used in this paper is  $\lambda_R = 0.493$  for a Rashba barrier with length  $100\text{nm}$ . This value of  $\lambda_R$  corresponds to Rashba spin splitting  $\Delta_R = 41.3\text{meV}$  which is not very large and theoretically can be obtained by using an appropriate substrate such as Au.<sup>40</sup> In addition, as mentioned before, to decrease the Rashba SOI strength, one can increase the Rashba barrier length [see Fig. 5(a)]. For instance, for a barrier

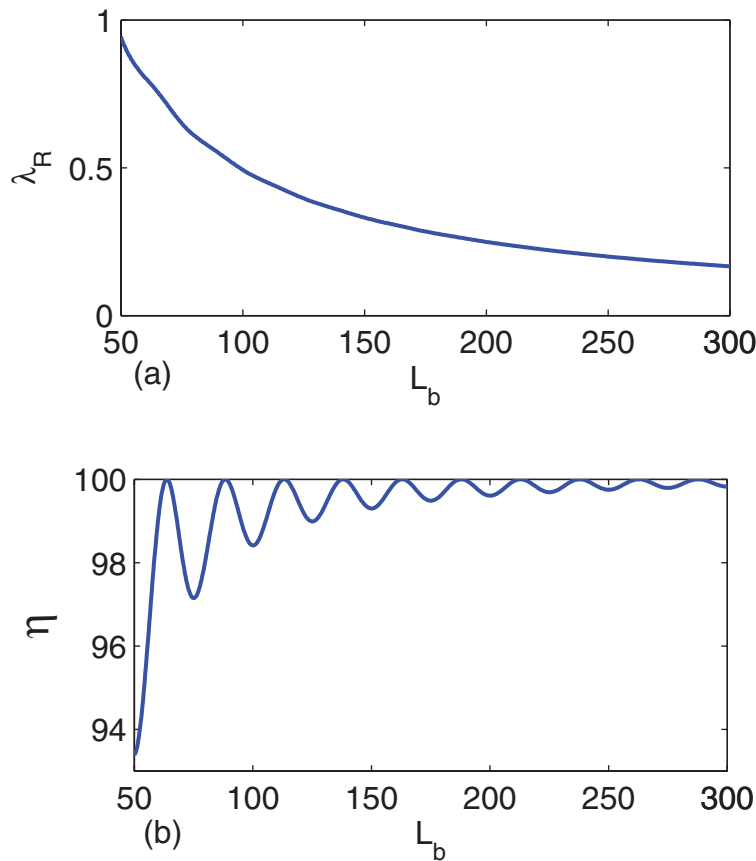


FIG. 5. (Color online) (a) Barrier height  $\lambda_R$  and (b) efficiency of spin-inverter  $\eta$  as a function of barrier length  $L_b$  for perfect spin inversion.

with length  $300\text{nm}$ , perfect spin-inversion can occur at Rashba spin splitting  $13.7\text{meV}$ . This value of Rashba spin splitting is feasible experimentally.<sup>38,39</sup>

#### IV. CONCLUSION

We have studied the spin-inversion properties of electron transmission in nanoscale graphene sheets with a Rashba spin-orbit barrier using transfer matrix method. Rashba SOI induces spin splitting in the electron energy which leads to spin-dependent transport in graphene sheets. It has been found that the electron complete spin-inversion can take place for proper values of barrier height or Rashba spin-orbit strength. The spin-inversion depends on the electron incident angle and complete spin-inversion occurs in a wide range of incident angles near the normal incident (i.e.,  $-15^\circ < \theta < 15^\circ$ ). In the case of complete spin-inversion, the graphene with a Rashba spin-orbit barrier can be considered as a perfect spin-inverter which can be used in the spintronic devices. The spin-inversion occurs at the same condition (or Rashba SOI strength) for both up and down spins. The efficiency of graphene spin-inverter has oscillatory behavior with respect to barrier length and has a number of maximums at which the efficiency can reach to 100%. The effects of intrinsic SOI of graphene sheet have been investigated and it is shown that the intrinsic SOI has no significant effect on the angular region and efficiency of spin-inverter. The spin-inversion for a trapezoidal barrier has also been studied and shown that there are no considerable differences for spin-inversion properties for trapezoidal and rectangular barriers except the efficiency of spin-inverter with trapezoidal barrier is slightly greater than that of rectangular one. The graphene spin inverter needs no external magnetic

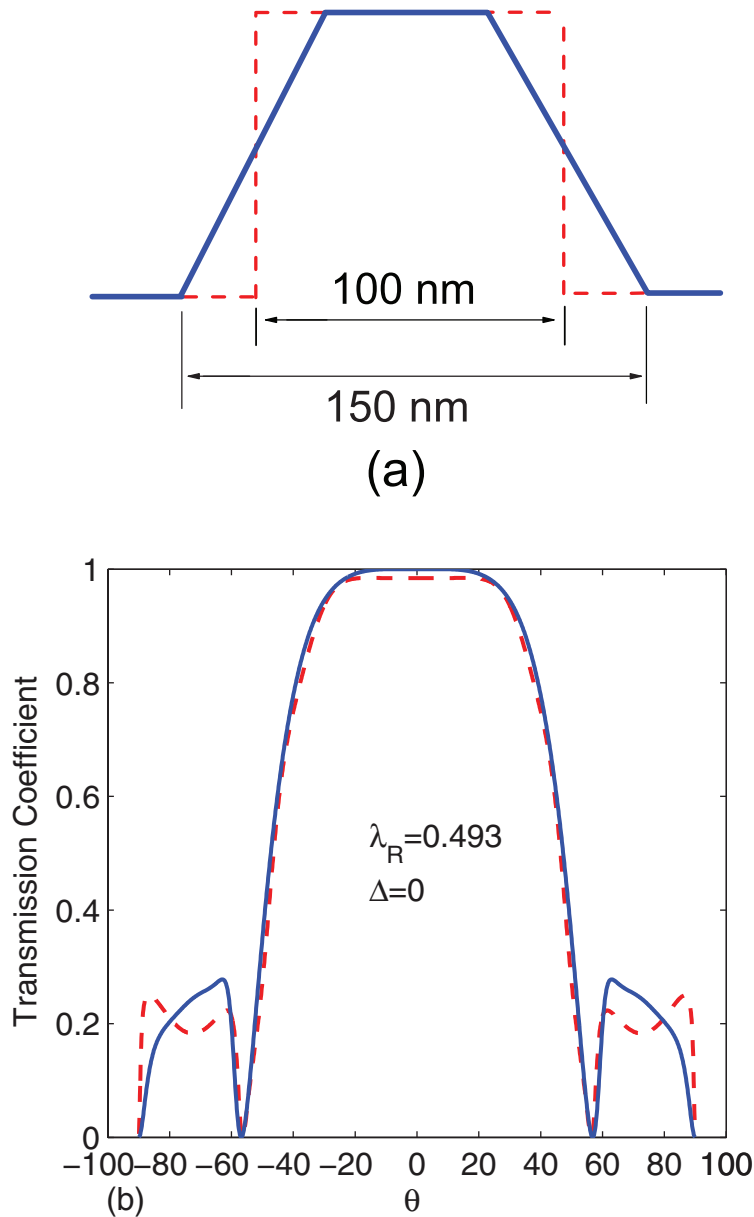


FIG. 6. (Color online) (a) A trapezoidal Rashba SOI barrier [blue (solid) lines] and a rectangular one [red (dashed) lines]. (b) Electron transmission coefficient with spin-inversion  $T_{\downarrow \rightarrow \uparrow}$  as a function of electron incident angle  $\theta$  for a trapezoidal barrier [blue (solid) curve] corresponding to Fig. 6(a). The electron transmission coefficient  $T_{\downarrow \rightarrow \uparrow}$  for a rectangular barrier is also shown in this figure [red (dashed) curve] for comparison.

or electric field. The results presented in this paper may be used to design of new carbon-based spintronic devices.

<sup>1</sup> Y. Zhang, Y. W. Tan, H. L. Stormer, and P. Kim, *Nature (London)* **438**, 197 (2005).

<sup>2</sup> K. S. Novoselov, E. McCann, S. V. Morozov, V. I. Fal'ko, M. I. Katsnelson, U. Zeitler, D. Jiang, F. Schedin, and A. K. Geim, *Nat. phys.* **2**, 177 (2006).

<sup>3</sup> K. Yang, *Solid State Commun.* **143**, 27 (2007).

<sup>4</sup> K. S. Novoselov, A. K. Geim, S. V. Morozov, D. Jiang, Y. Zhang, S. V. Dubonos, I. V. Grigorieva, and A. A. Firsov, *Science* **306**, 666 (2004).

<sup>5</sup> Y. Zhang, Y. W. Tan, H. L. Stormer, and P. Kim, *Nature (London)* **438**, 201 (2005).

- <sup>6</sup> K. S. Novoselov, A. K. Geim, S. V. Morozov, D. Jiang, M. I. Katsnelson, I. V. Grigorieva, S. V. Dubonos, and A. A. Firsov, *Nature (London)* **438**, 197 (2005).
- <sup>7</sup> K. Saito, J. Nakamura, and A. Natori, *Phys. Rev. B* **76**, 115409 (2007).
- <sup>8</sup> X. Li, X. Wang, L. Zhang, S. Lee, and H. Dai, *Science* **319**, 1229 (2008).
- <sup>9</sup> J.-W. Jiang, J.-S. Wang, and B. Li, *Phys. Rev. B* **79**, 205418 (2009).
- <sup>10</sup> D. L. Nika, S. Ghosh, E. P. Pokatilov, and A. A. Balandin, *Appl. Phys. Lett.* **94**, 203103 (2009).
- <sup>11</sup> A. K. Geim and K. S. Novoselov, *Nat. mater.* **6**, 183 (2007).
- <sup>12</sup> E. B. Sonin, *Phys. Rev. B* **77**, 233408 (2008).
- <sup>13</sup> I. W. Frank, D. M. Tanenbaum, A. M. Van Der Zande, and P. L. McEuen, *J. Vac. Sci. Technol. B* **25**, 2558 (2007).
- <sup>14</sup> C. Lee, X. Wei, J. W. Kysar, and J. Hone, *Science* **321**, 5887 (2008).
- <sup>15</sup> H. E. Romero, P. Joshi, A. K. Gupta, H. R. Guutierrez, M. W. Cole, S. A. Tadigadapa, and P. C. Eklund, *Nanotechnology* **6**, 652 (2007).
- <sup>16</sup> F. Schedin, A. K. Geim, S. V. Morozov, E. W. Hill, P. Blake, M. I. Katsnelson, and K. S. Novoselov, *Nat. Mater.* **6**, 622 (2007).
- <sup>17</sup> N. Tombros, C. Jozsa, M. Popinciuc, H. T. Jonkman, and B. J. van Wees, *Nature (London)* **448**, 571 (2007).
- <sup>18</sup> W. Han, R. K. Kawakami, *Phys. Rev. Lett.* **107**, 047207 (2011).
- <sup>19</sup> K. Pi, W. Han, K. M. McCreary, A. G. Swartz, Yan Li, and R. K. Kawakami, *Phys. Rev. Lett.* **104**, 187201 (2010).
- <sup>20</sup> T.-Y. Yang, J. Balakrishnan, F. Volmer, A. Avsar, M. Jaiswal, J. Sann, S. R. Ali, A. Pachoud, M. Zeng, M. Popinciuc, G. Guntherodt, B. Beschoten, and B. Ozyilmaz, *Phys. Rev. Lett.* **107**, 047206 (2011).
- <sup>21</sup> A. Saffarzadeh and M. Ghorbani Asl, *Eur. Phys. J. B* **67**, 239 (2009).
- <sup>22</sup> C. Bai, J. Wang, S. Jia and Y. Yang, *Physica E* **43**, 884 (2011).
- <sup>23</sup> A. Yamakage, K. -I. Imura, J. Cayssol, and Y. Kuramoto, *EPL*, **87**, 47005 (2009).
- <sup>24</sup> D. Bercieux and A. De Martino, *Phys. Rev. B* **81**, 165410 (2010).
- <sup>25</sup> V. H. Nguyen, A. Bournel, and P. Dollfus, *J. Appl. Phys.* **109**, 073717 (2011).
- <sup>26</sup> C. Bai, J. Wang, S. Jia and Y. Yang, *Appl. Phys. Lett.* **96**, 223102 (2010).
- <sup>27</sup> C. Cao, Y. Wang, H.-P. Cheng, and J. Jiang, *Appl. Phys. Lett.* **99**, 073110 (2011).
- <sup>28</sup> B. Zhou, X. Chen, B. Zhou, K.-H. Ding and G. Zhou, *J. Phys.: Condens. Matter* **23**, 135304 (2011).
- <sup>29</sup> Y. W. Son, M. Cohen, and S. G. Louie, *Nature (London)* **444**, 347 (2006).
- <sup>30</sup> T. O. Wehling, K. S. Novoselov, S. V. Morozov, E. E. Vdovin, M. I. Katsnelson, A. K. Geim, and A. I. Lichtenstein, *Nano Lett.* **8**, 173 (2008).
- <sup>31</sup> O. V. Yazyev and L. Helm, *Phys. Rev. B* **75**, 125408 (2007).
- <sup>32</sup> H. Haugen, D. Huertas-Hernando, and A. Brataas, *Phys. Rev. B* **77**, 115406 (2008).
- <sup>33</sup> D. Huertas-Hernando, F. Guinea, and A. Brataas, *Phys. Rev. B* **74**, 155426 (2006).
- <sup>34</sup> J. C. Boettger and S. B. Trickey, *Phys. Rev. B* **75**, 121402(R) (2007).
- <sup>35</sup> Y. Yao, F. Ye, X. L. Qi, S. -C. Zhang, and Z. Fang, *Phys. Rev. B* **75**, 041401(R) (2007).
- <sup>36</sup> H. Min, J. E. Hill, N. A. Sinitsyn, B. R. Sahu, L. Kleinman, and A. H. MacDonald, *Phys. Rev. B* **74**, 165310 (2006).
- <sup>37</sup> Yu. S. Dedkov, M. Fomon, U. Rudiger, and C. Laubschat, *Phys. Rev. Lett.* **100**, 107602 (2008).
- <sup>38</sup> O. Rader, A. Varykhalov, J. Sanchez-barriga, D. Marchenko, A. Rybkin, and A. M. Shikin, *Phys. Rev. Lett.* **102**, 057602 (2009).
- <sup>39</sup> A. Varykhalov, J. Sanchez-barriga, A. M. Shikin, C. Biswas, E. vescovo, D. Marchenko, A. Rybkin, and O. Rader, *Phys. Rev. Lett.* **101**, 157601 (2008).
- <sup>40</sup> Z. Y. Li, Z. Q. Yang, S. Qiao, J. Hu, and R. Q. Wu, *J. Phys.: Condens. Matter* **23**, 225502 (2011).
- <sup>41</sup> A. H. Castro Neto and F. Guinea, *Phys. Rev. Lett.* **103**, 157601 (2009).
- <sup>42</sup> J. L. Cardoso and P. Pereyra, *EPL*, **83**, 38001 (2008).
- <sup>43</sup> M. Busl and G. platero, *Phys. Rev. B* **82**, 205304 (2010).
- <sup>44</sup> F. Fallah and Esmailzadeh, *AIP Advances* **1**, 032113 (2011).
- <sup>45</sup> C. L. Kane and E. J. Mele, *Phys. Rev. Lett.* **95**, 226801 (2005).
- <sup>46</sup> K. S. Yi, D. Kim, and K. S. Park, *Phys. Rev. B* **76**, 115410 (2007).
- <sup>47</sup> B. H. J. McKellar and G. J. Stephenson, Jr., *Phys. Rev. C* **35**, 2262 (1987).
- <sup>48</sup> F. Zhai and H. Q. Xu, *Phys. Rev. Lett.* **94**, 246601 (2005).